LAWRENCE
LIVERMORE
NATIONAL
LABORATORY

UCRL-CONF-224052

Fast Prediction of HCCi Combustion with an Artificial Neural Network Linked to a Fluid Mechanics Code

S. M. Aceves, D. L. Flowers, J.-Y. Chen
A. Babaimopoulos

August 29, 2006

Fast Prediction of HCCI Combustion with an Artifical Neural Network Linked to a Fluid Mechanics Code
Toronto, Canada
October 16, 2006 through October 19, 2006

Disclaimer

2006-01-3298

Fast Prediction of HCCI Combustion with an Artificial Neural Network Linked to a Fluid Mechanics Code

Salvador M. Aceves, Daniel L. Flowers
Lawrence Livermore National Laboratory

J.-Y. Chen
University of California Berkeley

Aristotelis Babajimopoulos
University of Michigan

ABSTRACT

We have developed an artificial neural network (ANN) based combustion model and have integrated it into a fluid mechanics code (KIVA3V) to produce a new analysis tool (titled KIVA3V-ANN) that can yield accurate HCCI predictions at very low computational cost. The neural network predicts ignition delay as a function of operating parameters (temperature, pressure, equivalence ratio and residual gas fraction). KIVA3V-ANN keeps track of the time history of the ignition delay during the engine cycle to evaluate the ignition integral and predict ignition for each computational cell. After a cell ignites, chemistry becomes active, and a two-step chemical kinetic mechanism predicts composition and heat generation in the ignited cells.

KIVA3V-ANN has been validated by comparison with isooctane HCCI experiments in two different engines. The neural network provides reasonable predictions for HCCI combustion and emissions that, although typically not as good as obtained with the more physically representative multi-zone model, are obtained at a much reduced computational cost. KIVA3V-ANN can perform reasonably accurate HCCI calculations while requiring only 10% more computational effort than a motored KIVA3V run. It is therefore considered a valuable tool for evaluation of engine maps or other performance analysis tasks requiring multiple individual runs.

INTRODUCTION

Homogeneous Charge Compression Ignition (HCCI) combustion is a thermal autoignition process that initiates simultaneously at numerous sites before rapidly spreading throughout the combustion chamber [1, 2]. HCCI autoignition contrasts sharply with the turbulent flame propagation of SI engines and the mixing controlled combustion of diesel engines. This contrast has important consequences. HCCI Autoignition can be sustained even at very lean (ϕ < 0.2 [3]), or very dilute (EGR > 0.6 [4]) conditions, cooling combustion temperatures sufficiently to keep NO_x emissions extremely low (a few parts per million). If the HCCI combustion charge is lean and well mixed, very little particulate matter (PM) is produced. Furthermore, HCCI engines can approach the high efficiency of diesel engines because they can operate unthrottled at high compression ratio.

Spectroscopy experiments [1] and computer models [5] suggest that chemical kinetics dominates thermal autoignition in HCCI. Ignition begins in hot spots formed due to non-uniformities in temperature or concentration [6]. Unburned fuel and air are compressed and heated by the expansion of hot reaction products. Compression heating from the burned gases typically generates temperatures hot enough to combust the fuel (except for fuel in the crevices and boundary layers [7,8]), and is the main mechanism for spreading combustion in HCCI engines. Flame propagation (diffusion of energy and radicals from the burned zone to the unburned zone [9]) plays a secondary role in spreading combustion. This conclusion is supported by experimental results [10] that indicate that the speed of propagation of the combustion front in HCCI is far faster than deflagration in SI engines.

It is generally thought that turbulence plays an indirect role in HCCI combustion. Turbulence controls heat transfer to the cylinder walls, thereby establishing the temperature distribution in the cylinder. The temperature distribution determines the heat release rate. If the engine charge is isothermal, all the fuel autoignites simultaneously, combusting too rapidly. A broad temperature distribution has the desirable effect of slowing the combustion event.

Chemical kinetics is easier to characterize than turbulence, enabling detailed and accurate HCCI modeling with reduced computational expense relative to SI or diesel modeling. Still, the computational effort for HCCI modeling is substantial. For accurate HCCI analysis it is necessary to consider the effect of the temperature field on the ignition chemistry. This can be

accomplished at high computational expense with a full integration of a chemical kinetics code and a fluid mechanics code [11], or at reduced computational cost with a sequential integration of the codes through a multi-zone model [5]. Multi-zone models successfully predict HCCI combustion and emissions while reducing running time to ~2 days on single processor 2 GHz computers when working with high resolution engine meshes (~50,000 cells), 40 zones and detailed chemical kinetic mechanisms for long chain hydrocarbons, such as iso-octane (with ~800 species).

While multi-zone models have enabled inexpensive HCCI computations, it is important to develop faster solution techniques for accurate screening of multiple operating conditions. In this paper we describe the integration of a combustion model based on an artificial neural network (ANN) and a fluid mechanics code (KIVA3V) into a new analysis tool titled KIVA3V-ANN that delivers very fast HCCI computations while maintaining reasonable accuracy. This paper summarizes the details and validation of the model.

THE ARTIFICIAL NEURAL NETWORK (ANN)

The fundamentals of ANNs and their applicability to modeling combustion chemistry have been described in multiple publications [12-16]. Mathematically, the neural network is a universal approximator for non-linear functions that predicts an output value (or values) based on a set of input parameters and a training procedure. Our HCCI neural network (Figure 1 [17]) predicts ignition delay (τ) as a function of four input parameters: temperature (T), pressure (p), equivalence ratio (ϕ), and residual gas fraction (EGR). Ignition delay is defined as the time necessary for a fuel-air mixture to release 50% of the available chemical heat when kept at constant pressure. The ignition integral (Equation 1, [18]) predicts ignition based on the time history of ignition delay during a thermodynamic process (e.g., the compression stroke in an engine).

$$I(t) = \int_0^t \frac{1}{\tau(T, p, \phi, EGR)} dt \qquad (1)$$

It is typically considered that a mixture of fuel and air ignites when I(t)=1.

The neural network was trained for iso-octane by generating a set of ignition delay data with a chemical kinetics code (Chemkin [19]) and a detailed mechanism (859 species [20]). The neural network was trained to predict ignition delay over a wide range of conditions that cover the typical HCCI operating space:

600 K ≤ T ≤ 1500 K
1 bar ≤ P ≤ 200 bar
0.1 ≤ ϕ ≤ 0.45
0 ≤ EGR ≤ 0.2

Ignition delay was calculated for 38,880 points that cover the operating range with good resolution. Two thirds of the points were used for ANN training and a third for testing. Each individual run takes approximately 10 minutes in a 2 GHz Linux computer. Neural network training is a computationally intensive process that can be conducted in a reasonable time by running simultaneously on multiple processors.

We tuned several parameters to improve ANN accuracy. These parameters (and their optimum values) are the number of hidden layers (2), the number of nodes in hidden layer (20), and the epoch size (200). ANN training was carried out through the back-propagation algorithm [21].

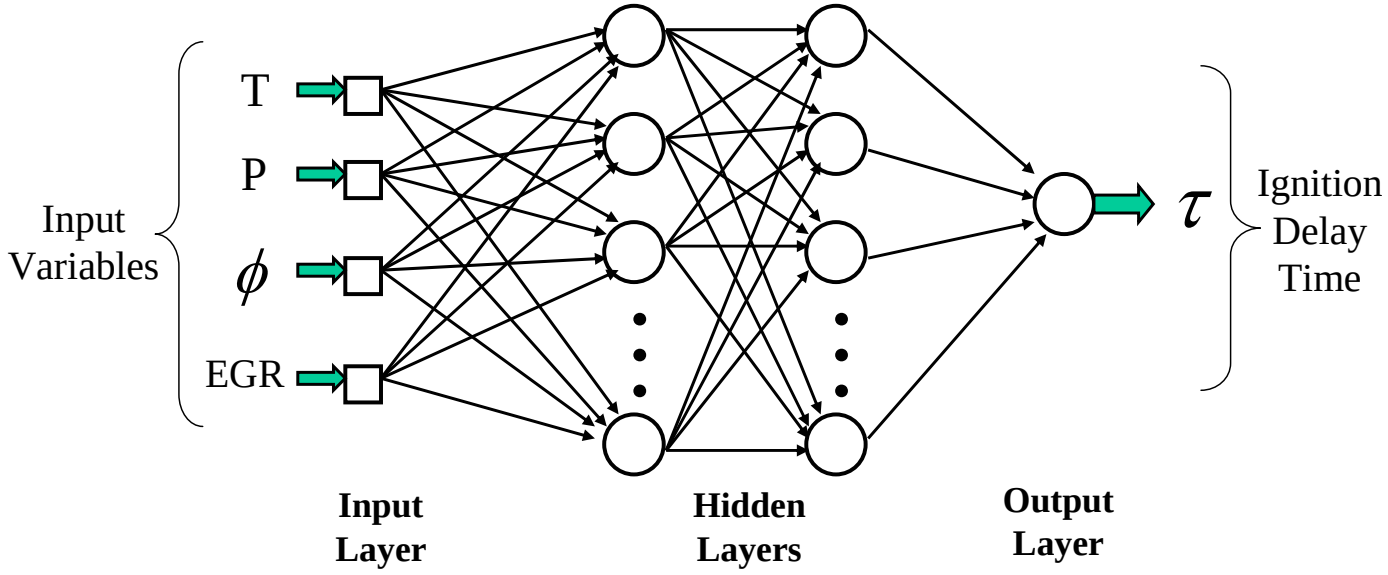

Figure I. Artificial neural net with four input variables, two hidden layers, and an output variable used for prediction of ignition delay

Table 1. Chemical kinetic constants and reaction rates used in KIVA3V-ANN for the forward and backward chemical reactions (Equations 2 and 3). C is the pre-exponential factor and E is the activation temperature (in K). The table also lists (in parentheses) two values for C originally proposed by Westbrook and Dryer [23] that were modified for KIVA3V-ANN.

Reaction	C	E	Reaction rate
Equation 2, forward	5.7×10^{11}	1.51×10^{4}	$C \exp(-E/T)[C_8H_{18}]^{0.25}[O_2]^{1.5}$
Equation 2, backward	0	0	0
Equation 3, forward	1.0×10^{10} (4.0×10^{14})	2.0×10^{4}	$C \exp(-E/T)[CO]^{1.0}[H_2O]^{0.5}[O_2]^{0.25}$
Equation 3, backward	5.0×10^{7} (5.0×10^{8})	2.0×10^{4}	$C \exp(-E/T)[CO_2]^{1.0}$

Table 2. Engine specifications and operating conditions for Volvo TD100 engine (Lund) and Cummins B engine (Sandia).

Engine	Volvo TD100	Cummins B
Displaced volume, cm^3	1600	981
Bore, mm	120.65	102
Stroke, mm	140	120
Connecting rod length, mm	260	192
Compression ratio	11.2:1	17.63:1
Exhaust valve open	39° BBDC	60° BBDC
Exhaust valve close	10° BTDC	8° ATDC
Inlet valve open	5° ATDC	3° BTDC
Inlet valve close	13° ABDC	25° ABDC
Compression ratio	11.2:1	17.63:1
Engine speed, rpm	1200	1200
Fuel	Iso-octane	Iso-octane
Equivalence ratio	0.4	0.04-0.26
Absolute intake pressure, bar	2	1.2

KIVA3V-ANN

The neural network incorporated into KIVA3V calculates ignition delay for every cell in the mesh, and KIVA3V-ANN calculates the ignition integral (Equation 1) during the engine cycle, without considering any diffusion or advection of the ignition integral between cells. When the ignition integral for a cell reaches a specified value (selected as I(t)=0.7 for best fit), combustion starts and the chemistry for the individual cell is activated. The ignition criterion is I(t)=0.7 instead of the typical I(t)=1.0 because the neural network was trained with 50% heat release data and is used within KIVA3V-ANN to predict the start of combustion. In addition to this, the mixture composition changes prior to the main combustion event due to pre-ignition chemistry. Ogink [22] showed that the ignition delay time for a mixture including intermediates and radicals can be significantly shorter than the ignition delay time based on the initial mixture composition at intake valve closing. KIVA3V-ANN does not consider pre-ignition chemistry, and therefore it is natural to expect I(t) < 1 at the ignition point.

Iso-octane combustion is calculated in the ignited cells with a 2-step mechanism [23]:

$$C_8H_{18} + 8.5O_2 \rightarrow 8CO + 9H_2O \quad (2)$$

$$CO + \tfrac{1}{2}O_2 \rightarrow CO_2 \quad (3)$$

Table 1 lists the chemical kinetic constants and reaction rates for the two reactions. We modified the two pre-exponential factors in the CO combustion reaction from the original values proposed by Westbrook and Dryer [23] to better match the experimental results. The original mechanism was developed for flame propagation and predicts extremely fast CO to CO_2 conversion under HCCI conditions. We did not conduct extensive tuning of the kinetic constants, and it may be possible to select optimum values that improve the quality of the experimental agreement.

KIVA3V-ANN is very efficient for conducting the chemistry calculations. A typical run with a 54,000 element mesh in a single processor 2 GHz Linux computer took ~4 hours, and only ~10% of this total time was spent on the neural network and chemistry subroutines. KIVA3V-ANN is only slightly more computationally intensive (~10%) than a motored run.

Figure 2. Flat piston crown used in the Lund experiment [24].

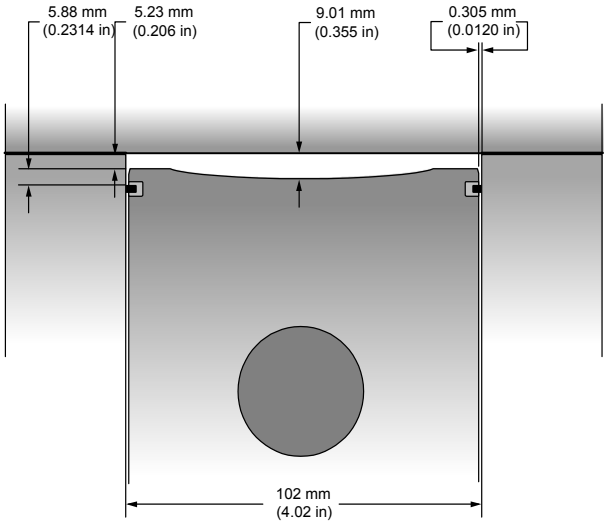

Figure 3. Schematic of the HCCI piston geometry and combustion chamber dimensions at TDC for the Sandia Cummins B engine [3].

EXPERIMENTS

KIVA3V-ANN was tested by comparison with two sets of experimental results that span a wide range of operating conditions (load, equivalence ratio, pressure, compression ratio). The first experiment was conducted at the Lund Institute of Technology and was part of a study on the effect of turbulence on HCCI combustion [24]. The experiment was done in a single cylinder of a Volvo™ TD100 truck engine. The engine specifications are shown in Table 2. The experiment was run supercharged at 2 bar absolute intake pressure with iso-octane fuel at 0.4 equivalence ratio, 11.2:1 compression ratio and 1200 rpm. Preheating of the intake air allowed adjustment of the ignition timing from early timing with steep pressure rise to very late timing with noticeable cycle-to-cycle variation. From the two geometries considered in [24], we only analyze the axisymmetric disc (flat top piston) cylinder geometry (Figure 2).

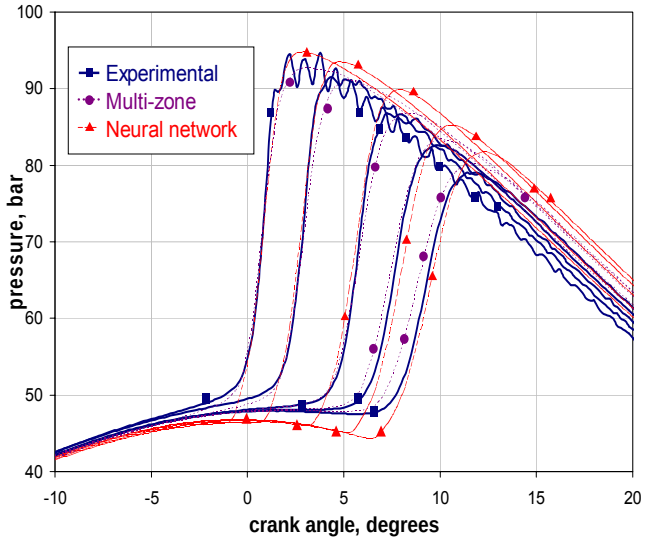

Figure 4. Pressure traces for the Lund experiment [24]. The figure shows experimental results (thick solid lines), multi-zone results (dotted lines) and neural network results (dashed lines).

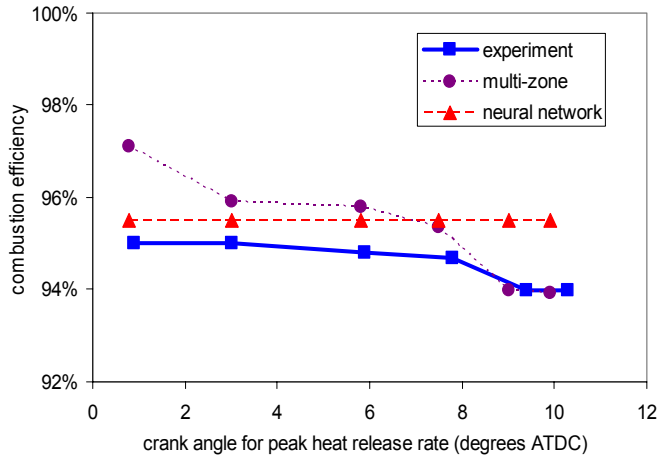

Figure 5. Combustion efficiency for the Lund engine. The figure shows experimental results (thick solid line), multi-zone results (dotted line) and neural network results (dashed line).

The second experiment was conducted at Sandia Livermore [3] to research HCCI operation at low loads. The engine used for this investigation is derived from a Cummins B-series medium-duty production diesel engine, with a displacement of 0.98 liters/cylinder. The engine is equipped with an axisymmetric custom piston shown schematically in Figure 3. This modified-pancake combustion chamber design provides a large squish clearance and a minimum top ring-land crevice volume, which amounts to only 1.4% of the top dead center (TDC) volume for the 17.63:1 compression-ratio piston used in this study. The experiments were conducted by keeping the ignition timing fixed at a few degrees before TDC while changing the equivalence ratio between 0.04 and 0.26. In this paper we only analyze the cases with $\phi \geq 0.10$ that fall within the range of the neural network training. The engine specifications and operating conditions are listed in Table 2.

Both experiments were previously analyzed by some of the authors with a multi-zone chemical kinetics model [8, 25]. This permits a comparison between the more physically representative multi-zone model and the faster neural network model. As a part of the previous analysis, we generated axisymmetric KIVA3V meshes for the two geometries. The meshes were carefully tested for grid size sensitivity and validated by comparison with motored data. The Lund engine mesh has 54,000 elements and the Sandia engine mesh has 51,000 elements.

RESULTS

Figure 4 shows pressure traces for the Lund experiment. The figure shows experimental results (thick solid lines), multi-zone results (dotted lines) and neural network results (dashed lines). The neural network predicts experimental pressure traces with reasonably good success, although the agreement is not as good as for the multi-zone model. The neural network does not account for low-temperature (cool flame) heat release, and therefore it underpredicts pressure in the initial stages of combustion. When ignition occurs, KIVA3V-ANN predicts a fast burn and overshoots the peak cylinder pressure, especially for the late burning cases.

The experimental and numerical combustion efficiencies for the Lund engine are compared in Figure 5. The figure shows that KIVA3V-ANN fits the experimental data better than the multi-zone model for the early combustion cases. However, the results hide the fact that the neural network greatly overpredicts CO emissions (~4100 ppm vs. 500 ppm for the experiment) and greatly undepredicts HC emissions (~70 ppm vs. ~2200 ppm for the experiment). The multi-zone model demonstrates better agreement in CO and HC emissions [25]. KIVA3V-ANN predicts constant combustion efficiency while experimental combustion efficiency drops as combustion is delayed. It must be noted that all hydrocarbon emissions predicted by KIVA3V-ANN are unreacted fuel, because no other HC is included in the 2-step kinetic mechanism. The multi-zone model does predict a wide range of intermediate and oxygenated hydrocarbons.

Figure 6 shows pressure traces for the Sandia experiment [3]. The figure shows experimental results (thick solid lines), multi-zone results (dotted lines) and neural network results (dashed lines). The figure shows a good agreement between KIVA3V-ANN and the experiments, especially for the higher equivalence ratios, where the neural network performs as well as the multi-zone model. However, the quality of agreement deteriorates as the equivalence ratio is reduced. For $\phi \leq 0.18$, KIVA3V-ANN overshoots the peak cylinder pressure. Once again, KIVA3V-ANN does not account for low-temperature heat release and underpredicts pressure in the early stages of combustion.

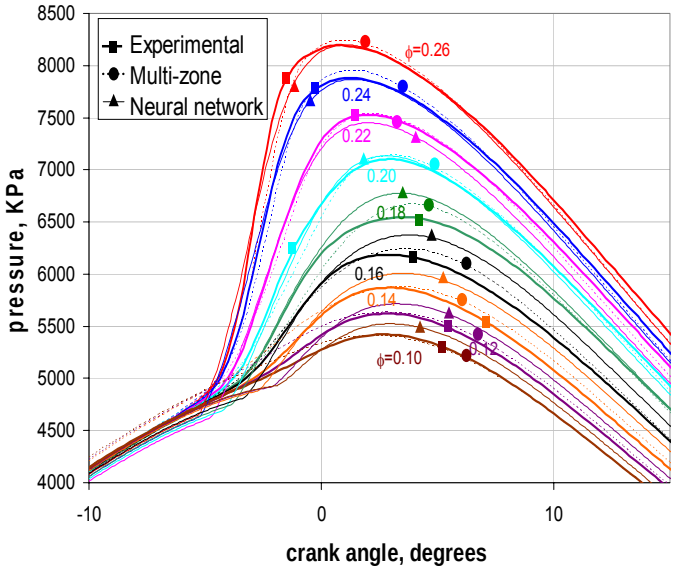

Figure 6. Pressure traces for the Sandia experiment. The figure shows experimental results (thick solid lines), multi-zone results (dotted lines) and neural network results (dashed lines).

The combustion efficiency comparison for the Sandia engine is shown in Figure 7. The neural network overpredicts the combustion efficiency at the lower equivalence ratios ($\phi \leq 0.22$), but it appropriately captures the reduction in combustion efficiency as the fuel-air mixture is made leaner. The multi-zone model shows better agreement with the experiments while also overpredicting the combustion efficiency at the lower equivalence ratios.

Figure 8 shows the speciation of the exhaust emissions for the Sandia engine. The figure shows the fraction of carbon in the fuel that goes into the different exhaust species: carbon dioxide (CO_2), carbon monoxide (CO), hydrocarbon (HC) and oxygenated hydrocarbons (OHC). The figure shows experimental results (thick solid lines), multi-zone results (dotted lines) and neural network results (dashed lines). The figure shows a reasonably good agreement between the neural network and the experiment. For CO_2 and CO, the neural network

predictions are nearly as good as obtained with the multi-zone model. The neural network underestimates HC emissions, and predicts no OHC, which are not present in the two-step chemical kinetic mechanism.

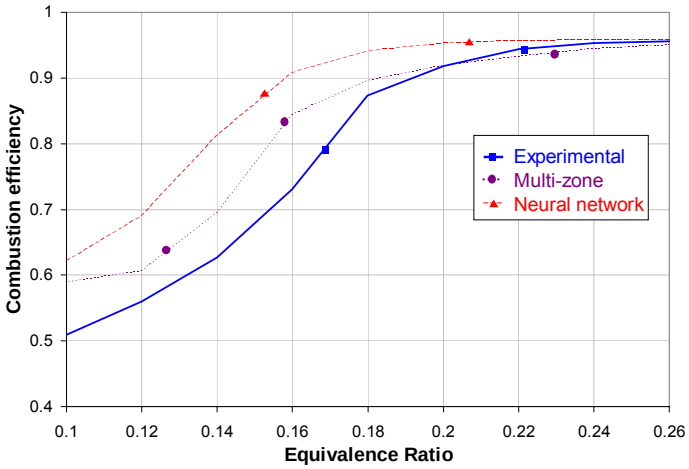

Figure 7. Combustion efficiency comparison for the Sandia engine. The figure shows experimental results (thick solid line), multi-zone results (dotted line) and neural network results (dashed line).

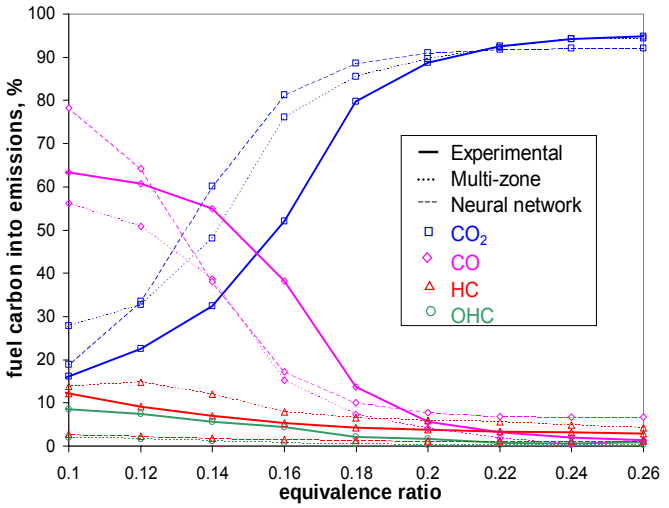

Figure 8. Speciation of the exhaust emissions for the Sandia engine. The figure shows the fraction of carbon in the fuel that goes into the different exhaust species: carbon dioxide (CO2), carbon monoxide (CO), hydrocarbon (HC) and oxygenated hydrocarbons (OHC). The figure shows experimental results (thick solid lines), multi-zone results (dotted lines), and neural network results (dashed lines). The neural network does not predict OHC because these are not included in the mechanism.

Figures 9-10 show a direct comparison between multi-zone [26] and neural network results for the Sandia engine with ϕ=0.20. This is one of the cases that produced the best agreement between the experimental results and the neural network (Figure 6), and it illustrates the main features and limitations of the model. The figures show mass fraction of fuel (Figure 9) and carbon monoxide (Figure 10) for six different crank angles that span most of the combustion process (between -8 and 10 crank angle degrees).

Comparing Figures 9 (a) and 9(b) we observe that the multi-zone model predicts earlier fuel decomposition (at -8° crank angle) in the central core (the hottest part of the cylinder). KIVA3V-ANN does not predict any low temperature heat release, and therefore fuel decomposition does not start until the main ignition takes place (at -4°). After this, combustion in the neural network proceeds quickly, and by TDC it has nearly caught up with the multi-zone model. In the late stages of combustion (4° to 10°) all the fuel reacts, except for the fuel trapped in the crevices. The multi-zone model considers partially reacted hydrocarbons in addition to just fuel, and therefore generates higher predictions of total hydrocarbon emissions than KIVA3V-ANN (Figure 8).

Figure 10 (b) shows that fuel decomposition in the multi-zone model does not immediately lead to CO. Instead, a long sequence of intermediate hydrocarbons are produced and then consumed in the path to CO and CO_2. This is in contrast with KIVA3V-ANN (Figure 10(a)) where the fuel immediately decomposes into CO with no intermediate steps (Equation 2). The neural network predicts peak CO production with good accuracy (at -2° crank angle) as well as CO decomposition into CO_2 (at TDC). The final stages of the combustion process are also accurately modeled with KIVA3V-ANN, which predicts that CO survives in the boundary layer near the cylinder liner, in agreement with the multi-zone model. The neural network accurately models the overall process of CO formation and decomposition, and the four last frames in Figures 10 (a) and 10 (b) are nearly identical.

CONCLUSIONS

This paper has described the development of an artificial neural network based combustion model and its training with a detailed isooctane mechanism to predict ignition delay as a function of operating parameters (temperature, pressure, equivalence ratio and residual gas fraction). KIVA3V-ANN keeps track of the time history of the ignition delay during the compression stroke to predict ignition for each computational cell. After a cell ignites, chemistry becomes active, and a two-step chemical kinetic mechanism predicts fuel decomposition and heat generation in the ignited cells. The main conclusions of the paper are:

1. KIVA3V-ANN has been validated by comparison with two HCCI experiments, and it provides reasonable predictions for HCCI combustion and emissions, although experimental agreement is typically not as good as obtained with the more physically representative and computationally intensive multi-zone model.

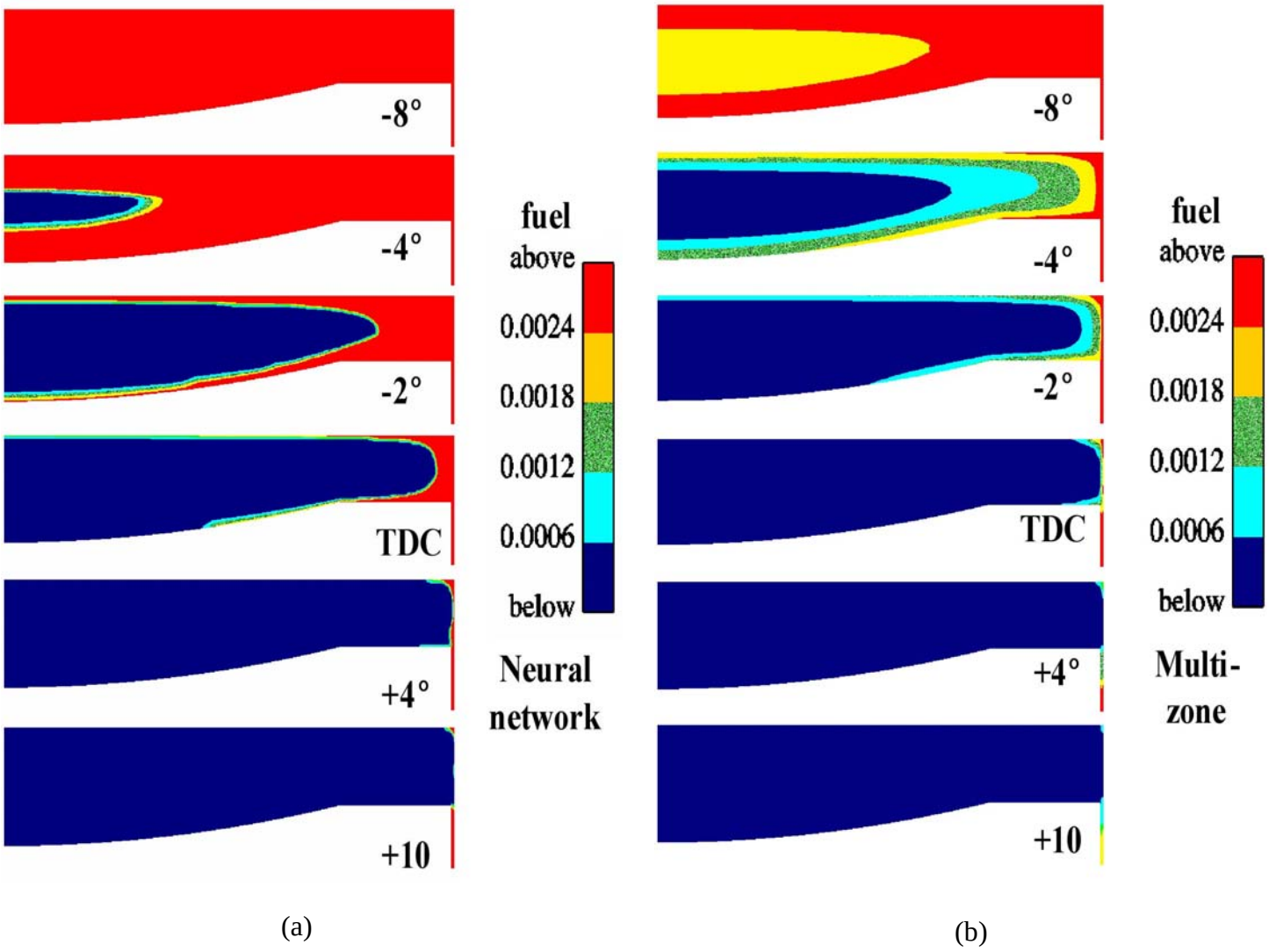

(a) (b)

Figure 9. Mass fraction of fuel in the cylinder of the Sandia engine for the case with ϕ=0.20 as predicted by (a) the neural network model and (b) the multi-zone model. The six frames in the figure illustrate the time history of fuel concentration in a period that spans most of the combustion process.

2. KIVA3V-ANN predicts fast combustion and often overpredicts the experimental peak cylinder pressure.

3. Combustion efficiency is well predicted by the neural network, although HC emissions are often underestimated and CO emissions are overestimated.

4. The current version of KIVA3V-ANN does not predict low-temperature heat release, and numerical pressure traces usually fall below experimental values in the early stages of combustion. KIVA3V-ANN still manages to make good predictions of pressure for the iso-octane HCCI cases analyzed here, but not predicting low-temperature heat release may introduce large errors when analyzing HCCI combustion of low octane fuels, such as n-heptane or diesel fuel.

5. KIVA3V-ANN can perform reasonably accurate HCCI calculations while requiring only 10% more computational effort than a motored KIVA3V run. It is therefore considered a valuable tool for evaluation of engine maps or other performance analysis tasks requiring multiple individual runs.

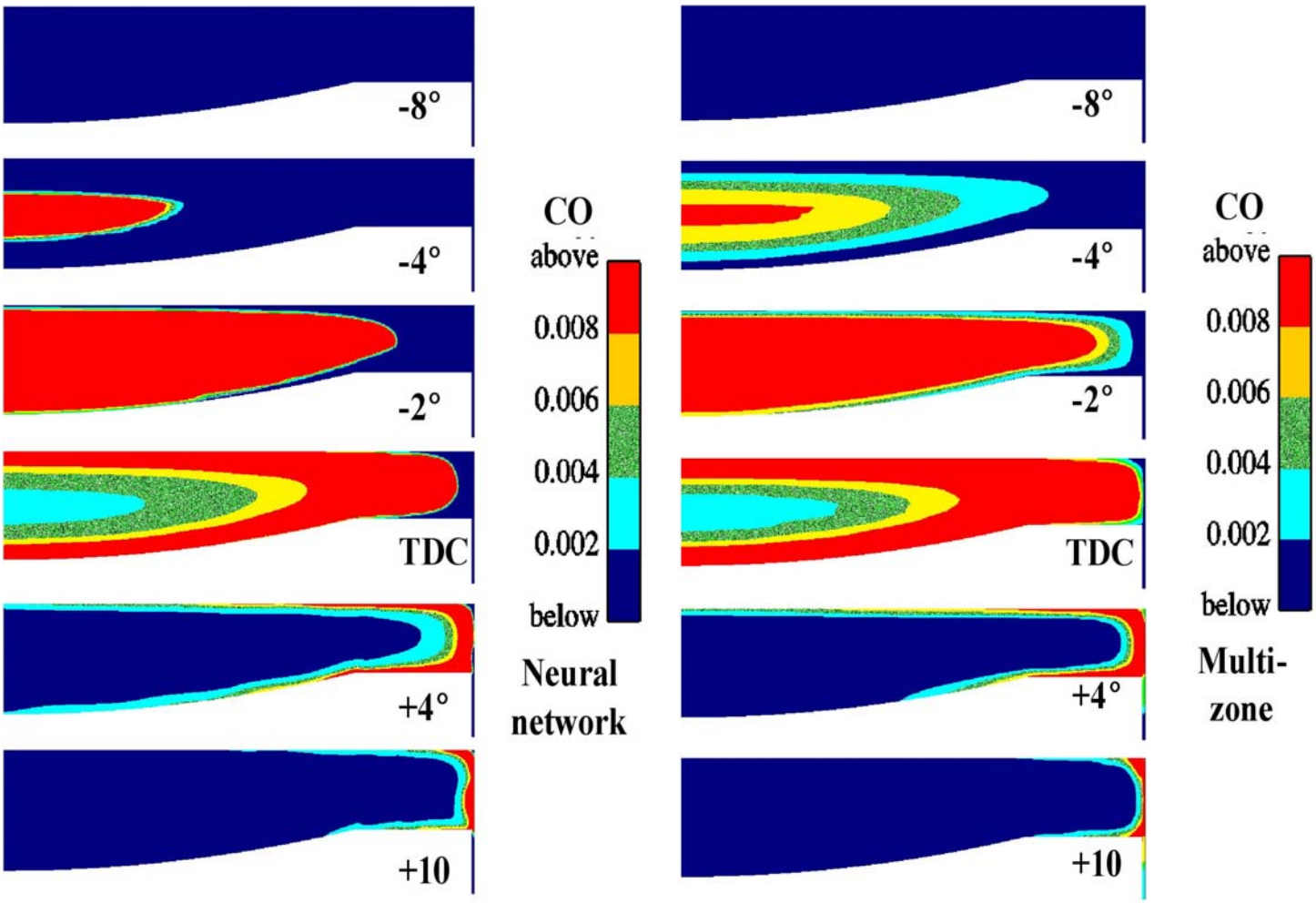

Figure 10. Mass fraction of carbon monoxide in the cylinder of the Sandia engine for the case with ϕ=0.20 as predicted by (a) the neural network model and (b) the multi-zone model. The six frames in the figure illustrate the time history of CO concentration in a period that spans most of the combustion process.

ACKNOWLEDGMENTS

This project is funded by DOE, Office of FreedomCAR and Vehicle Technologies, Kevin Stork and Gurpreet Singh, program managers. Additional funding from the DOE University Consortium on Low Temperature Combustion for High Efficiency, Ultra-Low Emission Engines, DE- FC26-06NT42629. Work performed under the auspices of the U.S. Department of Energy by University of California, Lawrence Livermore National Laboratory under Contract W-7405-ENG-48.

REFERENCES

1. Onishi, S., Jo, S. H., Shoda, K., Jo, P. D., and Kato, S., "Active Thermo-Atmosphere Combustion (ATAC) - A New Combustion Process for Internal Combustion Engines," SAE paper 790501, 1979.

2. Noguchi, M., Tanaka, Y., Tanaka, T., and Takeuchi, Y., "A Study on Gasoline Engine Combustion by Observation of Intermediate Reactive Products during Combustion," SAE paper 790840, 1979.

3. Dec, J.E., and Sjöberg, M. "A Parametric Study of HCCI Combustion – the Sources of Emissions at Low Loads and the Effects of GDI Fuel Injection," SAE Paper 2003-01-0752, 2003.

4. Oakley, A., Zhao, H., Ma, T., and Ladommatos, N., "Dilution Effects on the Controlled Auto-Ignition (CAI) Combustion of Hydrocarbon and Alcohol Fuels," SAE Paper 2001-01-3606, 2001.

5. Aceves, S. M., Flowers, D.L., Westbrook, C.K., Smith, J. R., Pitz, W.J., Dibble, R., Christensen, M. and Johansson, B., "A Multi-Zone Model for Prediction of HCCI Combustion and Emissions," SAE Paper 2000-01-0327, 2000.

6. Warnatz, J., Maas, U., and Dibble, R.W., "Combustion," 2nd Edition, Springer-Verlag, Berlin, 1999.

7. Aceves, S.M., Flowers, D.L., Espinosa-Loza, F., Martinez-Frias, J., Dibble, R.W., Christensen, M., Johansson, B., and Hessel, R.P., "Piston-Liner Crevice Geometry Effect on HCCI Combustion by Multi-Zone Analysis," SAE Paper 2002-01-2869, 2002.

8. Aceves, S.M., Flowers, D.L., Espinosa-Loza, F., Martinez-Frias, J., Dec, J.E., Sjöberg, M., Dibble, R.W., and Hessel, R.P., "Spatial Analysis of Emissions Sources for HCCI Combustion at Low Loads Using a Multi-Zone Model," SAE Paper 2004-01-1910, 2004.

9. Turns, S.R., An Introduction to Combustion, Concepts and Applications, Chapter 8, McGraw-Hill, New York, NY, 2000.

10. Hultqvist, A., Christensen, M., Johansson, B., Richter, M., Nygren, J., Hult, J., and Alden, M., "The HCCI Combustion Process in a Single Cycle-High-Speed Fuel Tracer LIF and Chemiluminescence Imaging, SAE Paper 2002-01-0424, 2004.

11. Kong, S.C., Reitz, R.D., Christensen, M., and Johansson, B., "Modeling the Effects of Geometry-Generated Turbulence on HCCI Engine Combustion," SAE Paper 2003-01-1088, 2003.

12. Christo, F.C., Masri, A.R., and Nebot, E.M., "Integrated PDF/neural network approach for simulating turbulent reacting systems," Combustion and Flame, Vol. 106, pp. 406-421, 1996.

13. Blasco, J.A., Fueyo, N., Dopazo, C., and Ballester, J., "Modelling the temporal evolution of a reduced combustion chemical system with an artificial neural network," Combustion and Flame, Vol. ll3, pp. 38-52, 1998.

14. Blasco, J.A., Fueyo, N., Larroya, J.C., Dopazo, C., and Chen, J.-Y., "Single-step time-integrator of a methane-air chemical system using artificial neural networks," Computers and Chemical Engineering, Vol. 23, pp. 1l27-1133, 1999.

15. Chen, J.-Y., Blasco, J.A., Fueyo, N., and Dopazo, C., "An economical strategy for storage of chemical kinetics: Fitting in situ adaptive tabulation with artificial neural networks," Proceedings of the Combustion Institute, Vol. 28, pp. ll5-121, 2001.

16. He, Y., and Rutland, C.J., "Application of Artificial Neural Networks in Engine Modeling," International Journal of Engine Research, Vol. 5, pp. 281-296, 2004.

17. Choi, Y., and Chen, J.-Y., "Fast Prediction of Start of Combustion in HCCI with Combined Artificial Neural Networks and Ignition Delay Model," Proceedings of the Combustion Institute, Vol. 30, pp. 2711-2718, 2005.

18. Livengood, J.C., and Wu, P.C., "Correlation of Autoignition Phenomenon in Internal Combustion Engines and Rapid Compression Machines," Proceedings of the Combustion Institute, Vol. 5, pp. 347-356, 1955.

19. Kee, R.J., Rupley, F.M., Meeks, E., and Miller, J.A., "CHEMKIN III: A FORTRAN Chemical Kinetics Package for the Analysis of Gas-Phase Chemical and Plasma Kinetics," Sandia National Laboratories Report SAND96-8216, Livermore, CA, 1996.

20. Curran, H. J., Gaffuri, P., Pitz, W. J., and Westbrook, C. K., "A Comprehensive Modeling Study of Iso-Octane Oxidation," Combustion and Flame, Vol. 129, pp. 253-280, 2002.

21. Rumelhart, D.E., Hinton, G.E., and Williams, R.J., "Learning representations by back--propagating errors," Nature, Vol. 323, pp. 533-536, 1986.

22. Ogink, R., "Approximation of Detailed-Chemistry Modeling by a Simplified HCCI Combustion Model," Paper 2005-24-37, Proceedings of the 7th SAE International Conference on Engines for Automobile, ICE2005, Capri, Italy, 2005.

23. Westbrook, C.K., and Dryer, F.L., "Simplified Mechanisms for the Oxidation of Hydrocarbon Fuels in Flames," Combustion Science and Technology, Vol. 27, pp. 31-43, 1981.

24. Christensen, M., Hultqvist, A., and Johansson, B., "The Effect of Combustion Chamber Geometry on HCCI Operation," SAE Paper 2002-01-0425, 2002.

25. Aceves, S.M., Flowers, D.L., Espinosa-Loza, F., Martinez-Frias, J., Christensen, M., Johansson, B., and Hessel, R., "Analysis of the Effect of Geometry Generated Turbulence on HCCI Combustion by Multi-Zone Modeling," SAE Paper 2005-01-2134.

26. Flowers, D.L., Aceves, S.M., and Babajimopoulos, A., "Effect of Charge Non-uniformity on Heat Release and Emissions in PCCI Engine Combustion," SAE Paper 2006-01-1363, 2006.